Journal of Clinical and Translational Hepatology **2023** vol. 11(6) | 1308–1320
DOI: 10.14218/JCTH.2023.00184

Original Article

IGF2BP3 Enhances the Growth of Hepatocellular Carcinoma Tumors by Regulating the Properties of Macrophages and CD8$^+$ T Cells in the Tumor Microenvironment

Lingyu Ma, Jiayu Jiang, Qin Si, Chong Chen and Zhaojun Duan*

Department of Immunology, Institute of Basic Medical Sciences, Chinese Academy of Medical Sciences, School of Basic Medicine, Peking Union Medical College, Beijing, China

Received: 21 April 2023 | **Revised:** 26 May 2023 | **Accepted:** 21 June 2023 | **Published online:** 1 August 2023

Abstract

Background and Aims: Overexpression of IGF2BP3 is associated with the prognosis of hepatocellular carcinoma (HCC). However, its role in regulating tumor immune microenvironment (TME) is not well characterized. Here, we investigated the effects of IGF2BP3 on macrophages and CD8$^+$ T cells within the TME of HCC. ***Methods:*** The relationship between IGF2BP3 and immune cell infiltration was analyzed using online bioinformatics tools. Knockout of *IGF2BP3* in mouse hepatoma cell line Hepa1-6 was established using CRISPR/Cas9 technology. *In vitro* cell coculture and subcutaneously implanted hepatoma mice model were used to explore the effects of IGF2BP3 on immune cells. Expression of CCL5 or transforming growth factor beta 1 (TGF-β1) was detected with quantitative real-time polymerase chain reaction, western blotting, and enzyme-linked immunosorbent assay. The binding of IGF2BP3 and its target RNA was verified by trimolecular fluorescence complementation system and RNA immunoprecipitation followed by quantitative or semiquantitative polymerase chain reaction. ***Results:*** IGF2BP3 expression was elevated in HCC and was positively correlated with macrophage infiltration. Patients with higher IGF2BP3 expression and lower macrophage infiltration had a better survival rate. We found that IGF2BP3 could bind to the mRNA of CCL5 or TGF-β1, increasing their expression, and inducing macrophage infiltration and M2 polarization while inhibiting the activation of CD8$^+$ T cells. Furthermore, inhibition of IGF2BP3 combined with anti-CD47 antibody treatment significantly suppressed the growth of hepatoma in Hepa1-6 xenograft tumor mice. ***Conclusions:*** IGF2BP3 promoted the infiltration and M2-polarization of macrophages and suppressed CD8$^+$ T activation by enhancing CCL5 and TGF-β1 expression, which facilitated the progression of Hepa1-6 xenograft tumor.

Keywords: Hepatocellular carcinoma; IGF2BP3; TGF-β1; CCL5; M2 macrophage; CD8$^+$ T cell.

Abbreviations: CRISPR/Cas9, clustered regularly interspaced short palindromic repeat/Cas9 endonuclease; ELISA, Enzyme-linked immunosorbent assay; HCC, hepatocellular carcinoma; PBS, phosphate buffered saline; RBP, RNA binding protein; RIP, RNA immunoprecipitation; TME, tumor immune microenvironment; TriFc, trimolecular fluorescence complementation.

***Correspondence to:** Zhaojun Duan, Department of Immunology, Institute of Basic Medical Sciences, Chinese Academy of Medical Sciences, School of Basic Medicine, Peking Union Medical College, 5 Dongdan Sansan, Dongcheng District, Beijing 100005, China. ORCID: https://orcid.org/0000-0001-6530-3158. Tel/Fax: +86-10-69156475, E-mail: duanzhaojun@ibms.pumc.edu.cn

Citation of this article: Ma L, Jiang J, Si Q, Chen C, Duan Z. IGF2BP3 Enhances the Growth of Hepatocellular Carcinoma Tumors by Regulating the Properties of Macrophages and CD8$^+$ T Cells in the Tumor Microenvironment. J Clin Transl Hepatol 2023;11(6):1308–1320. doi: 10.14218/JCTH.2023.00184.

Introduction

Hepatocellular carcinoma (HCC) is the most commonly diagnosed primary liver cancer. The complex immune environment in liver cancer has a crucial role in the progression of this disease.[1,2] Macrophages are important regulators of the tumor immune microenvironment (TME).[3] In general, macrophages can polarize into two distinct phenotypes, the classically activated M1 macrophages and the alternative activated M2 macrophages. M1 macrophages have pro-inflammatory and antitumor activity, while M2 macrophages suppress inflammation and participate in angiogenesis.[4,5] Available evidence suggests that tumor-associated macrophages have an M2-like phenotype and are associated with poor prognosis in many malignancies.[6–8] In HCC, M2 macrophages facilitate the migration and invasion of tumor cells and are usually associated with a poor prognosis.[3,9] Various cytokines and proteases secreted by M2 macrophages are involved in the inhibition of CD8$^+$ T cells, tumor neovascularization, and tumor metastasis.[10]

IGF2BP3, located on chromosome 7p15.3 in humans, is weakly expressed in normal adult tissue but is dramatically elevated during carcinogenesis.[11–13] It activates signal pathways related to cell growth and promotes the differentiation, proliferation, invasion, and metastasis of HCC cells.[14–18] In colon cancer, IGF2BP3 acts as a N^6-methyladenosine reader to regulate the tumor cell cycle.[19] IGF2BP3 also promotes the expression of drug resistance genes, leading to drug resistance of tumors.[20] However, there is a paucity of studies investigating the role of IGF2BP3 in regulating immune cells within the TME. Bioinformatics analysis showed that high IGF2BP3 expression in clinical bladder cancer tissues was associated with the infiltration of multiple immune cells, including neutrophils and macrophages.[21] Additionally, bioinformatics analysis indicated that N^6-methyladenosine-related gene clusters, including IGF2BP3, were closely associated with the infiltration of a variety of immune cells in HCC, including fol-

licular helper T cells and macrophages.[22] The results suggest a potential regulatory role of IGF2BP3 in the immune microenvironment of HCC. However, further study is required to obtain more definitive evidence. In this study, we explored the role of IGF2BP3 in the tumor immune microenvironment of HCC. The focus of the study was to investigate the effects of IGF2BP3 on immune cells including macrophages as well as CD8$^+$ T cells. We also investigated the key molecules and mechanisms mediating the function of IGF2BP3.

Methods

Bioinformatics analysis

Bioinformatic analysis was performed using publicly available data from various databases. The expression of IGF2BP3 in liver cancer and corresponding normal tissues was analyzed with the GEPIA2 online tool (http://gepia2.cancer-pku.cn/#index). In addition, its expression at the single-cell level in the HCC tumor microenvironment was investigated using TISCH (http://tisch.comp-genomics.org/home/). IGF2BP3 expression in HCC samples at different stages and grades was analyzed on TISIDB (http://cis.hku.hk/TISIDB/). The relationship between IGF2BP3 expression and infiltration of various immune cells was analyzed in CAMOIP (https://www.camoip.net/). The association of the infiltration level of macrophages combined with IGF2BP3 expression and the overall survival rate of HCC patients was evaluated using TIMER (http://cistrome.org/TIMER/). The correlation between IGF2BP3 and immunosuppressive markers was analyzed in the TCGA HCC dataset (https://portal.gdc.cancer.gov/) (n=371).

Cell lines and reagents

Raw264.7 mouse macrophage cells and Hepa1-6 mouse hepatoma cells were obtained from the American Type Culture Collection (Manassas, VA, USA). Cells were cultured in Dulbecco's modified Eagle's medium (06-1055-57-1A; Biological Industries, Los Angeles, CA, USA) supplemented with 10% fetal bovine serum (10099-141; Thermo Fisher Scientific, Waltham, MA, USA) and 1% penicillin and streptomycin (15140122; Thermo Fisher Scientific). Cells were cultured at 37°C and 5% CO_2.

Construction of plasmids

The clustered regularly interspaced short palindromic repeat/Cas9 endonuclease (CRISPR/Cas9) was used to knock out *Igf2bp3* in Hepa1-6 cells. Plasmids containing gRNAs (TTCGTGGACTGCCCGGACGAGGG or AGACACTTTCCAGGTCCGCGGGG) targeting murine *Igf2bp3* were purchased from Ubigene_Bio and transfected into the Hepa1-6 cells. Cells successfully transfected were labeled with enhanced green fluorescent protein and sorted into single cells. Single clones were collected to confirm the knockout efficiency. The original plasmid of the trimolecular fluorescence complementation (TriFC) system was a gift from Professor Zongqiang Cui (State Key Laboratory of Virology, Wuhan Institute of Virology, Chinese Academy of Sciences, Wuhan 430071, China), and the plasmids were constructed as previously described.[23] The *Ccl5*-7 or *Tgf-β1*-28 fragment, which had been screened by RNA immunoprecipitation, was cloned into the pECFP-C1-ms2 plasmids, namely pECFP-C1-MS2-*Ccl5*-7 or pECFP-C1-MS2-*Tgf-β1*-28. The coding sequence of *Igf2bp3* was inserted into the pMN155 plasmid, namely p*Igf2bp3*-MN155.

Animal model and treatment

The animal study was approved by the Ethics Review Committee of the Peking Union Medical College (Beijing, China). Six-week-old, male C57BL/6J mice were purchased from Beijing Vital River Laboratory Animal Technology Co. Ltd. (Beijing, China). Briefly, 5×10^6 Hepa1-6 *Igf2bp3* wild-type and *Igf2bp3* knockout cells were subcutaneously implanted in the right flank of each mouse. Tumor size was measured starting on day 5, and the mice were sacrificed on day 18 after inoculation. For treatment experiment, tumor-bearing mice were administered intraperitoneal injection of anti-CD47 mAb (400 μg per mouse) (BE0270; Bio X Cell, Lebanon, NH, USA) on the seventh day after tumor implantation and then every 3 days for a total of five doses.

Western blotting

To extract total protein, cells were lysed with RIPA lysis and extraction buffer (89901; Thermo Fisher Scientific), followed by centrifugation at 13,000 *g* for 15 m. Protein concentration was determined with Pierce Rapid Gold bicinchoninic acid assay kits (A53226; Thermo Fisher Scientific) and the protein samples were resolved by sodium dodecyl-sulfate polyacrylamide gel electrophoresis and transferred to 0.22 μm polyvinylidene difluoride membranes (1620177; Bio-Rad, Hercules, CA, USA). Membranes were blocked with 5% bovine serum albumin for 1.5 h and the membranes were incubated overnight with primary antibodies against IGF2BP3 (ab177477; Abcam, Cambridge, UK), TGF-β1 (ab215715; Abcam), CCL5 (AF5151; Affinity Biosciences, Cincinnati, OH, USA), ARG1 (A1847; ABclonal, Woburn, MA, USA), and NOS2 (A14031; ABclonal) at 4°C. The next day, the membranes were washed and incubated with secondary antibodies for 1 h, and read using a high-sig enhanced chemiluminescence western blotting substrate (180-5001; Tanon Science & Technology Co, Ltd, Shanghai, China). Band quantification was performed with ImageJ software.

Enzyme-linked immunosorbent assay (ELISA)

Tumor cell culture supernatants were collected by centrifugation. Mouse TGF-β1 ELISA kits (EK981-96; MultiSciences, Bellingham, WA, USA) and mouse CCL5/RANTES ELISA kits (EK2129/2-96; MultiSciences) were used to determine the concentration of TGF-β1 and CCL5.

T-cell cytotoxicity

Ninety-six-well plates were precoated with CD3 (1 μg/mL) antibody 1 day in advance. Splenocytes from Hepa1-6-bearing C57BL/6J mice were lysed and centrifuged to prepare single-cell suspensions and CD8$^+$ T cells were isolated following the instructions included with EasySep mouse CD8$^+$ T-cell isolation kits (19853; STEMCELL, Vancouver, Canada). The CD8$^+$ T cells were stimulated and activated for 48 h by addition of CD28 antibody (2 μg/mL) and recombinant mouse interleukin (IL)-2 (10 ng/mL). The CD8$^+$ T cells were then cocultured with tumor cells at ratios of 1:1, 2:1, 4:1, 5:1, 8:1 and 10:1 for 5 h. The cells were collected for flow cytometry assay.

Migration assay

For migration assays, Raw264.7 cells (1×10^6 cells/mL) were seeded in 100 μL DMEM (1% FBS) onto 8 μm pore size polycarbonate filter membranes in 24-well plates. Tumor cell culture supernatant was added to the well beneath the membrane. After 48-h incubation, nonmigrating cells on the upper surface of the membrane were gently removed with a cotton swab. The cells that had migrated to the lower surface of the membrane were fixed and stained with 0.1% crystal violet for 10 m. After washing with phosphate buffered saline (PBS)

three times, the top chamber was dried with a cotton swab and photographed using a light microscope.

Immunofluorescence

Cells and tumor sections were fixed in 4% paraformaldehyde solution followed by immunohistochemical staining using standard procedures and the following antibodies: ARG1 (1:200; A1847; ABclonal), NOS2 (1:200; A14031; ABclonal), CD206 (1:1,000; ab64693; Abcam).

RNA extraction and real-time quantitative PCR (qRT-PCR)

Total RNA was extracted by Trizol reagent (A33252; Thermo Fisher Scientific) and first-strand cDNA was synthesized using HiScript II Q RT SuperMix reagent (R223-01; Vazyme Biotech, Nanjing, Jiangsu, China). qRT-PCR was conducted with qPCR Master Mix (Q311-02; Vazyme). The primers used are listed in Supplementary Table 1.

Flow cytometry

To prepare for surface staining, cells were diluted in PBS with 2% FBS to a concentration of 10^6 cells per 100 μL and incubated with fluorescently labeled antibodies for 30 m at 4°C. After surface staining, intracellular staining was performed with incubation in fixation buffer and permeabilization (88-8824-00; eBioscience, San Diego, CA, USA), followed by the staining protocol described above. Cells were washed and collected using Accuri C6 Plus (BD Biosciences, Franklin Lakes, NJ, USA) and data were analyzed with FlowJo software (version 10). The following antibodies (all from Biolegend, San Diego, CA, USA) were used: CD3 (100205), CD8 (100705), CD45 (103129), F4/80 (123125), CD206 (162505), I-A/I-E (MHCII) (107605), CD11b (101205), CD4 (100407), Gr-1 (108411), CD19 (152403), and NK1.1 (156507).

RNA immunoprecipitation (RIP)

For RNA immunoprecipitation, cells were lysed and the RNA was extracted with Magna RIP kits (17-700; Millipore, Burlington, MA, USA). The efficiency of immunoprecipitation was determined by western blotting. The quality of input RNA was measured with a NanoDrop spectrophotometer.

Novel far-red fluorescence complementation

Expression vectors were cotransfected into 293T cells with Lipofectamine 2000 reagent (Invitrogen, Waltham, MA, USA). According to the manufacturer's protocol,[23] transfected cells were incubated at 37°C in 5% CO_2 for 5–6 h and then at 30°C in 5% CO_2 for 18–24 h until imaging. Cells were imaged with a Leica DMi8 inverted microscope.

Statistical analysis

Results were reported as mean±SD, normality distribution was established, and GraphPad Prism 9 software was used for the statistical analysis. Student's *t*-test was used for comparison between groups and *p*-values <0.05 was considered significant.

Results

Expression of IGF2BP3 is increased in HCC and is positively correlated with macrophage infiltration

We first analyzed the expression of IGF2BP3 in clinical HCC samples through GEPIA2. Simultaneously, we used the immunohistochemistry data from the Human Protein Atlas portal (https://www.proteinatlas.org/) to observe the protein expression of IGF2BP3 in HCC (Fig. 1A). We found that the expression of IGF2BP3 in tumor tissue was significantly higher than that in normal tissue (p<0.05). Then, we assessed the expression of IGF2BP3 in individual cells of HCC from TISCH. The results revealed that IGF2BP3 was mainly expressed in malignant tumor cells (Supplementary Fig. 1A). We further used TISIDB website to analyze the expression of IGF2BP3 in HCC tissues with different pathologic stages (p=3.61e-03) and histologic grades (p=1.26e-05); the results demonstrated that the expression of IGF2BP3 increased with HCC progression (Fig. 1B). Next, we used CAMOIP and TIMER to investigate the potential correlation of IGF2BP3 with immune cell infiltration in HCC (Fig. 1C–D, Supplementary Fig. 1B). The findings indicated a positive relationship between macrophage infiltration and IGF2BP3 expression. We also observed that the group with high IGF2BP3 expression and high macrophage infiltration had significantly poorer survival than the group with high IGF2BP3 expression and low macrophage infiltration (p=0.0212; Fig. 1E). Collectively, the data demonstrate a positive association between IGF2BP3 and infiltration of macrophages.

IGF2BP3 facilitates macrophage migration and polarization in vitro

To verify whether IGF2BP3 promoted macrophage migration *in vitro*, we generated stable *Igf2bp3*-knockout Hepa1-6 cells with specific gRNA1 and gRNA2 (*Igf2bp3*_ko1 and *Igf2bp3*_ko2) by using the CRISPR/Cas9 technology. The knockout efficiency was validated by qRT-PCR (p<0.001) and western blotting (Fig. 2A). We then examined the migration of Raw264.7 after treatment with different tumor cell culture supernatants using Transwell assays. The results showed significant reduction in macrophage migration after stimulation by the supernatant of *Igf2bp3* knockout cells compared with that of *Igf2bp3*_wt (*Igf2bp3*_wild-type) Hepa1-6 cells (Fig. 2B) (p<0.001). We chose *Igf2bp3*_ko1 for the next study, named *Igf2bp3*_ko. Previous bioinformatics analysis had found a correlation of *IGF2BP3* expression with macrophage infiltration, and infiltration of M2 macrophages has been reported to promote HCC progression.[9] Therefore, it was hypothesized that tumor-cell derived IGF2BP3 was critical in M2 polarization. We conducted qRT-PCR to evaluate the expressions of M1 (*Nos2*, *Il-1β*, *Tnf-α*, *Cxcl9*) and M2 (*Arg1*, *Ccl22*) macrophage relevant markers in Raw264.7 cells after stimulation with culture supernatants of *Igf2bp3*_wt and *Igf2bp3*_ko cells for 48 hours. The results showed that M1 markers, *Nos2* (p<0.01), *Il-1β* (p<0.001), *Tnf-α* (p<0.01), and *Cxcl9* (p<0.05) were increased while M2 marker, *Arg1* (p<0.01), and *Ccl22* (p<0.05) were decreased after stimulation with *Igf2bp3*_ko cell supernatant (Fig. 2C). Western blotting results showed that ARG1 decreased while NOS2 increased after stimulation with *Igf2bp3*_ko cell supernatant (Fig. 2D). The same results were observed on cell immunofluorescence staining (Fig. 2E). Collectively, the data indicated that IGF2BP3 in tumor cells promoted migration and M2 polarization of macrophages.

IGF2BP3 promotes tumor progression and facilitates macrophage infiltration and polarization in mouse HCC model

As IGF2BP3 has been shown to promote macrophage migration and polarization *in vitro*, we explored the situation *in vivo*. C57BL/6J mice were given a subcutaneous injection of 5×10^6 *Igf2bp3*_wt or *Igf2bp3*_ko cells and the tumor growth was monitored. We observed that after knocking out *Igf2bp3* in Hepa1-6 cells, the tumor volume increased much slower than it did in the wild-type group (Fig. 3A)

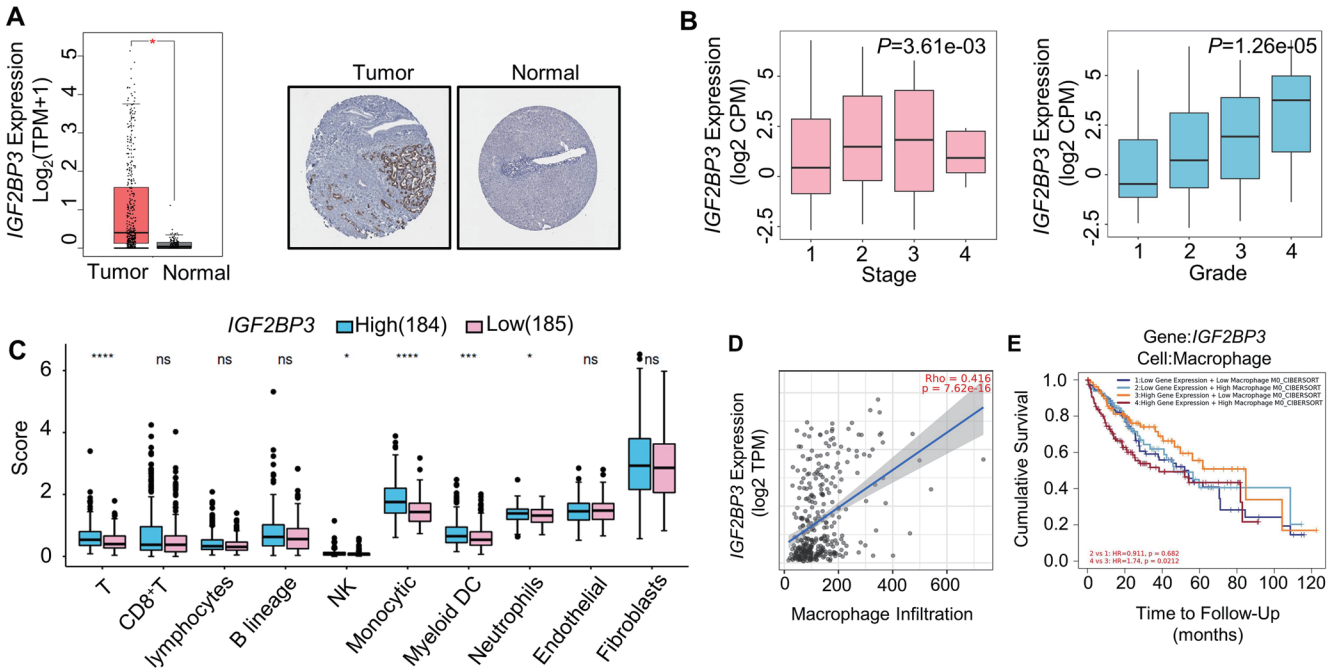

Fig. 1. Expression of IGF2BP3 is increased in HCC and is positively correlated with the infiltration of macrophages. (A) The expression of IGF2BP3 in liver cancer and corresponding normal tissues was analyzed using the GEPIA2 (left). The ordinate, $\log_2$ (TPM+1) is transformed from expression data for differential analysis. The protein expression of IGF2BP3 in liver cancer and corresponding normal tissues in The Human Protein Atlas (right). (B) Analysis of the IGF2BP3 expression in HCC samples of different stages and grades in TISIDB website based on the TCGA database. The ordinate, $\log_2$CPM, represents read counts converted using the Voom method. (C) Correlation between IGF2BP3 expression and immune cell infiltration in CAMOIP. (D) Association of macrophage infiltration level with IGF2BP3 in HCC analyzed in TIMER. (E) Survival curves showing the effects of IGF2BP3 expression and macrophages on overall survival in TCGA HCC sample via TIMER2. *p<0.05, ***p<0.001, ****p<0.0001; ns, not significant. HCC, hepatocellular carcinoma.

and tumor weight was significantly reduced (p<0.01; Fig. 3B). The knockout group also showed improved survival (p=0.001; Fig. 3C). We then analyzed the infiltrating immune cells in tumor tissue and found that the proportion of CD11b⁺monocytes (p<0.05), total F4/80⁺macrophages (p<0.05), and F4/80⁺CD206⁺ M2 macrophages (p<0.05) was significantly lower in *Igf2bp3*_ko tumors than in *Igf2bp3*_wt tumors (Fig. 3D). Immunofluorescence staining revealed a significant reduction (p<0.01) in CD206⁺ cells in *Igf2bp3*_ko tumors (Fig. 3E). The findings suggested that IGF2BP3 promoted macrophage infiltration and polarization. Interestingly, as shown in Figure 3D, we also observed greater infiltration of CD3⁺ T (p<0.01), CD4⁺ T (p<0.01), CD8⁺ T (p<0.05), F4/80⁺MHCII⁺ M1 macrophages (p<0.01), CD19⁺ B (p<0.001), and NK1.1⁺ NK (p<0.001) cells in the *Igf2bp3*_ko tumors than in the *Igf2bp3*_wt tumors. However, the infiltration of CD11b⁺Gr-1⁺ myeloid-derived suppressor cells (p<0.01) in *Igf2bp3*_ko tumors was less than that in the *Igf2bp3*_wt tumors, suggesting that IGF2BP3 induced a suppressive tumor immune microenvironment. Collectively, the data suggest that IGF2BP3 promoted tumor progression and facilitated infiltration and M2-polarization of macrophages in the mouse HCC model.

IGF2BP3 facilitates macrophage infiltration and polarization by promoting the secretion of CCL5 and TGF-β1 from tumor cells

Cytokines have an important role in the infiltration of immune cells. Macrophage infiltration and M2 polarization can be induced by CCL5 and TGF-β1, respectively.[24,25] Based on those studies, we examined CCL5 and TGF-β1 expression in *Igf2bp3*_wt and *Igf2bp3*_ko cells (Fig. 4A–C). The results showed that the expression and secretion of CCL5 and TGF-β1 were lower in *Igf2bp3*_ko cells than in *Igf2bp3*_wt cells. The results of ELISA and immunohistochemical staining of the tumor tissue were consistent (Fig. 4D–E). We next investigated whether IGF2BP3 regulated the infiltration of macrophages through CCL5. Transwell assays detected the migration of macrophages stimulated by supernatants from *Igf2bp3*_wt cells, *Igf2bp3*_ko cells, *Igf2bp3*_ko cells with added CCL5, CCL5 only and supernatants from *Igf2bp3*_wt cells with added anti-CCL5, *Igf2bp3*_wt cells with added IgG. Consistent with previous finding, the number of migrating cells induced by supernatant from *Igf2bp3*_ko cells was reduced compared with the *Igf2bp3*_wt group. Adding CCL5 to the supernatant of *Igf2bp3*_ko cells increased cell migration (p<0.001; Fig. 4F). However, blockade of CCL5 by anti-CCL5 antibody in the supernatant of *Igf2bp3*_wt cells attenuated the migration induced by the supernatant of *Igf2bp3*_wt cells (p<0.001; Fig. 4G). The results suggest that tumor-cell derived IGF2BP3 promoted recruitment of macrophages by promoting the secretion of CCL5. To investigate whether IGF2BP3 promoted M2 polarization through TGF-β1, supernatants of *Igf2bp3*_wt cells, *Igf2bp3*_ko cells, *Igf2bp3*_wt cells with anti-TGF-β1, and *Igf2bp3*_wt cells with IgG were added to Raw264.7 cell cultures. Macrophages were collected after 48 h and markers, including Nos2, IL6, H2-Ab1, Tnf-α (M1), Arg1, IL10, and Ym1 (M2) were detected by qRT-PCR. As shown in Figure 4H, when the *Igf2bp3*_wt group was treated with TGF-β1 neutralizing antibody, the expression of M2 macrophage markers, Arg1 (p<0.01), Il-10 (p<0.01), and Ym1 (p<0.001) were significantly decreased compared with the *Igf2bp3*_wt group. The findings suggest that IGF2BP3 facilitated macrophage infil-

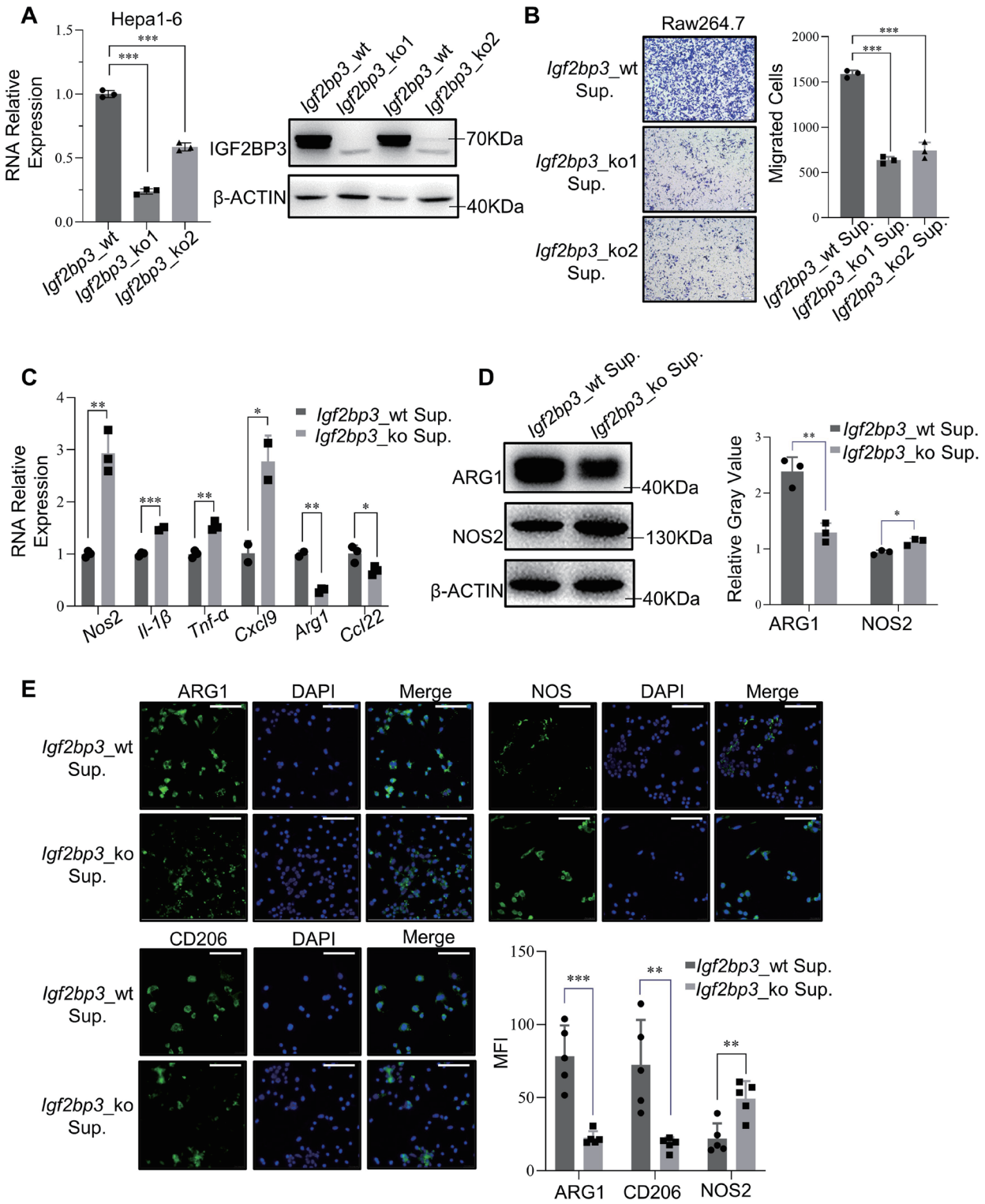

Fig. 2. IGF2BP3 facilitates macrophage migration and polarization *in vitro*. (A) Results of qRT-PCR and western blots confirming the knockout of *Igf2bp3*. (B) Transwell chamber assay of the migration of Raw264.7 cells after treatment with the supernatant from *Igf2bp3*_wt and *Igf2bp3*_ko cells. The graph shows the number of cells per field of view. Scale bar=100 μm. (C) qRT-PCR results showing relative M1 (nos2, Il-1β, Tnf-α, Cxcl9) and M2 (Arg1, Ccl22) gene expression levels in Raw264.7 cells after treatment with the supernatant from *Igf2bp3*_wt and *Igf2bp3*_ko cells. (D) Western blot assay of cell lysates from Raw264.7 cells after treatment with the supernatant from *Igf2bp3*_wt and *Igf2bp3*_ko cells. (E) Immunofluorescence staining of ARG1, CD206, and NOS2 in Raw264.7 cells after treatment with the supernatant from *Igf2bp3*_wt and *Igf2bp3*_ko cells. The histogram shows the mean fluorescence intensity of both groups. Scale bar=100 μm. wt, wild-type; ko, knockout; *Igf2bp3*_wt Sup., *Igf2bp3*_wt cell culture supernatants; *Igf2bp3*_ko Sup., *Igf2bp3*_ko cell culture supernatants. Data are mean±SD. **p*<0.05, ***p*<0.01, ****p*<0.001.

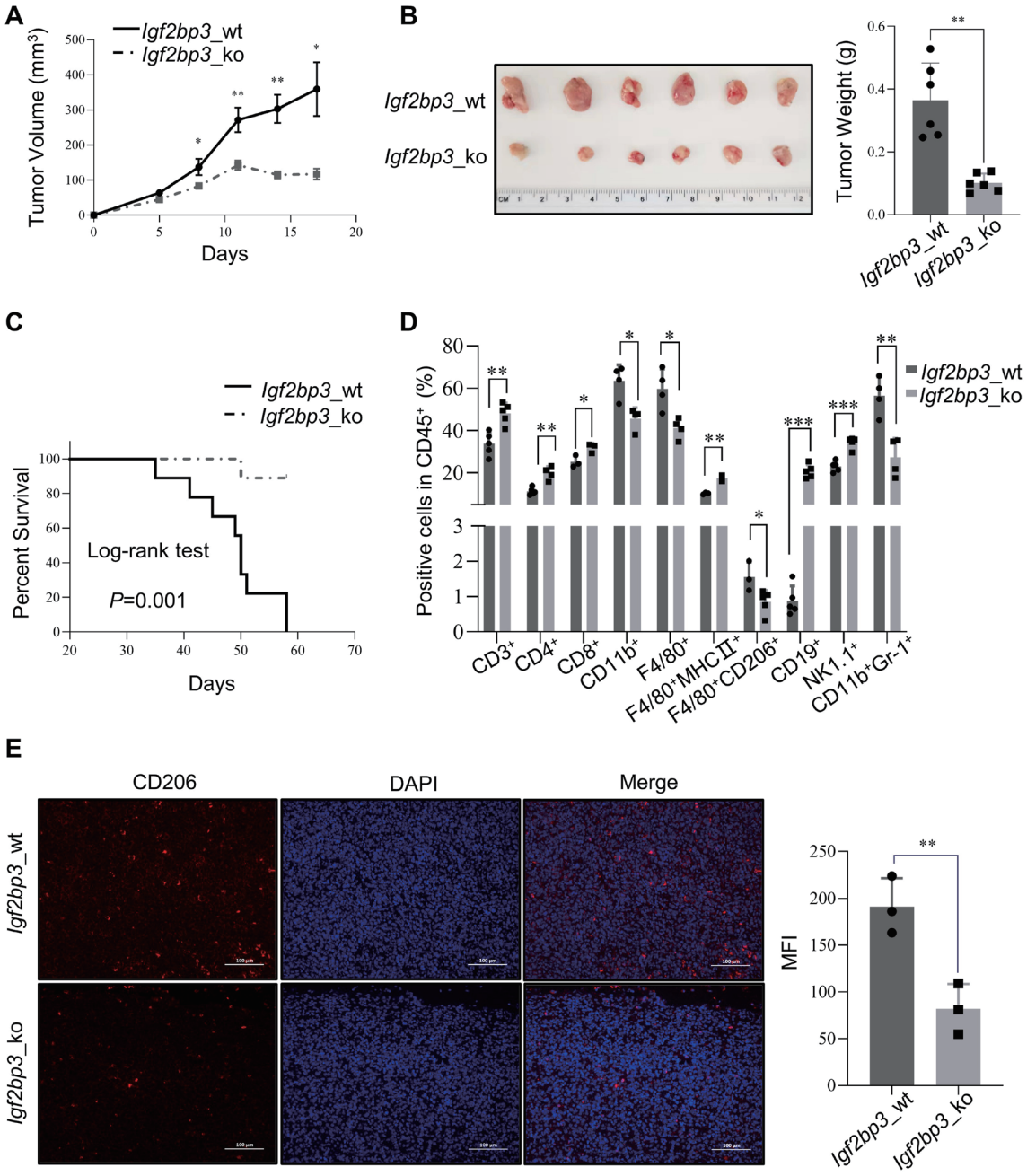

Fig. 3. IGF2BP3 promotes tumor progression and facilitates macrophage infiltration and polarization in mouse HCC model. *Igf2bp3*_wt and *Igf2bp3*_ko cells were subcutaneously injected in 6-week-old, male C57BL/6J mice. (A) Tumor volume was measured and recorded every 3 days from initial injection to tumor harvest. (B) Image of the harvested tumors (left), mice were sacrificed on day 21, tumor weight was recorded (right). (C) Kaplan–Meier survival curves of mice bearing *Igf2bp3*_wt and *Igf2bp3*_ko tumors. Log-rank tests were used to assess between-group differences in survival. (D) Percentages of $CD3^+$, $CD4^+$, $CD8^+$, $CD11b^+$, $F4/80^+$, $F4/80^+MHCII^+$, $F4/80^+CD206^+$, $CD19^+$, $NK1.1^+$ and $CD11b^+Gr\text{-}1^+$ cells in *Igf2bp3*_wt and *Igf2bp3*_ko tumors. (E) Images of CD206 immunofluorescence staining for tissue sections of *Igf2bp3*_wt and *Igf2bp3*_ko tumors (left) and quantified as mean fluorescence intensity per high power field (right). Scale bar=100 μm. Data are mean±SD. **p*<0.05, ***p*<0.01, ****p*<0.001. HCC, hepatocellular carcinoma.

tration and M2-polarization by promoting the secretion of CCL5 and TGF-β1 by tumor cells.

IGF2BP3 inhibits the activation of $CD8^+$ T cells by promoting the secretion of TGF-β1

The TGF-β signaling pathway is known to have a critical role in inhibiting $CD8^+$ T cytotoxicity.[26] Therefore, we downloaded and analyzed the transcriptome data of HCC patients from the TCGA database and found that IGF2BP3 was positively correlated with immunosuppressive factors of tumor cells and factors of exhausted T-cell phenotypes (Fig. 5A). Thus, we hypothesized that IGF2BP3 in tumors may inhibit the activation of $CD8^+$ T cells by promoting TGF-β1 expression. To test the hypothesis, splenocytes of Hepa1-6 tumor-bearing

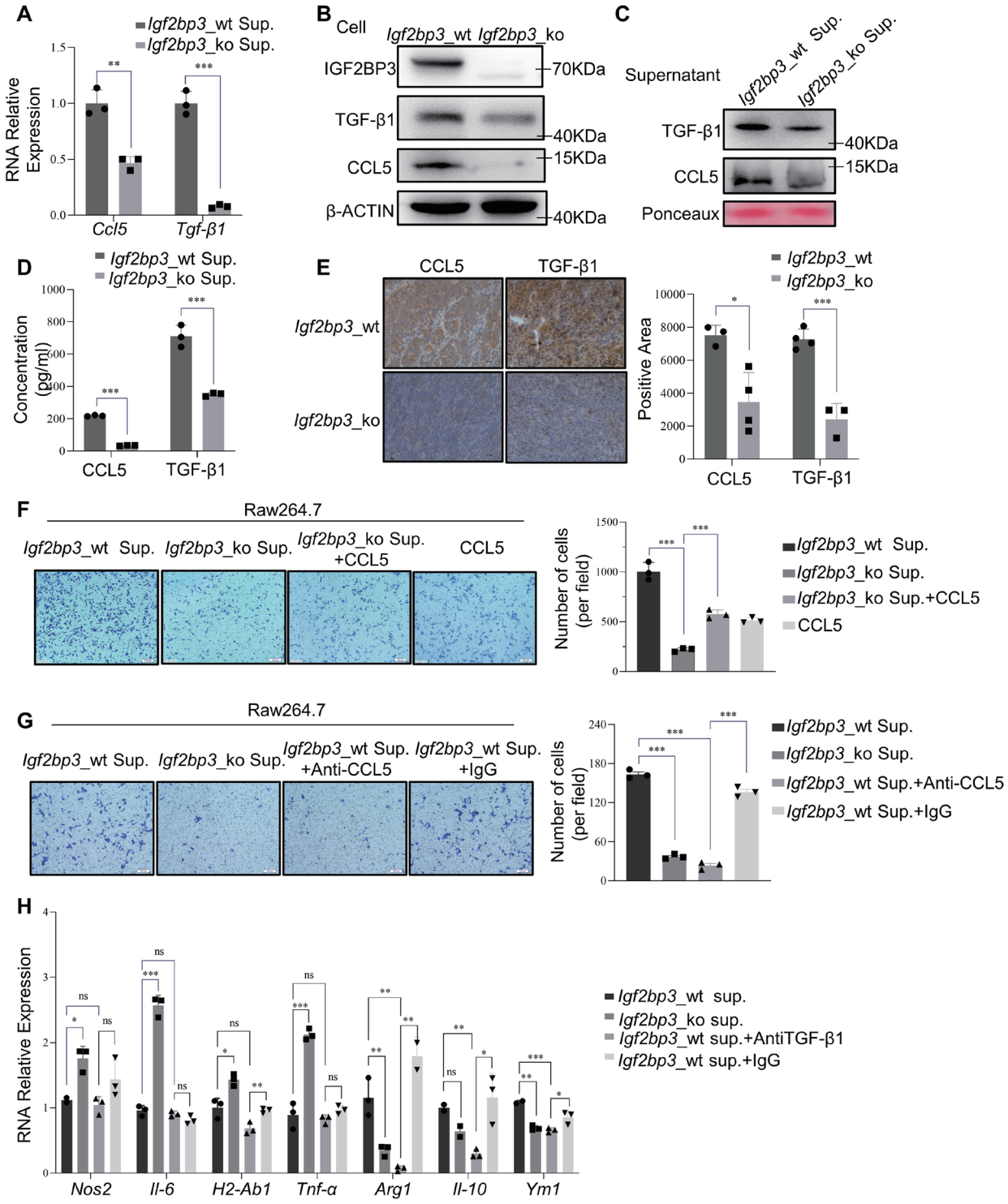

Fig. 4. IGF2BP3 facilitates macrophage infiltration and polarization by promoting the secretion of CCL5 and TGF-β1 from tumor cells. (A–C) qRT-PCR (A) and western blots showing the expression of CCL5 and TGF-β1 in *Igf2bp3*_wt and *Igf2bp3*_ko cells (B) and culture supernatants (C). (D) ELISA results showing the levels of CCL5 and TGF-β1 in Hepa1-6 cell culture supernatant. (E) Immunohistochemical (IHC) staining for CCL5 and TGF-β1 expression in *Igf2bp3*_wt and *Igf2bp3*_ko tumor tissue (left); the histogram summarizes the staining intensity (right). Scale bar=50 μm. (F, G) Transwell assay performed with Raw264.7 cells. Cells were suspended in serum-free media and seeded into the upper chamber. Cell culture supernatant was added to the lower chamber. CCL5 (100 ng/mL), Anti-CCL5 (200 ng/mL). The histogram summarizes the migration results. The graph shows the number of cells per field of view. Scale bar=100 μm. (H) *Igf2bp3*_wt cells were cultured with TGF-β1 neutralizing antibody (1 μg/mL). Raw264.7 cells stimulated with tumor supernatant. The *H2-Ab1*, *Tnf-α*, *Arg1*, and *Il-10* expression in Raw264.7 cells was determined by qRT-PCR. *Igf2bp3*_wt Sup., *Igf2bp3*_wt cell culture supernatants; *Igf2bp3*_ko Sup., *Igf2bp3*_ko cell culture supernatants. Data are mean±SD. *p<0.05, **p<0.01, ***p<0.001. ns, not significant. ELISA, Enzyme-linked immunosorbent assay.

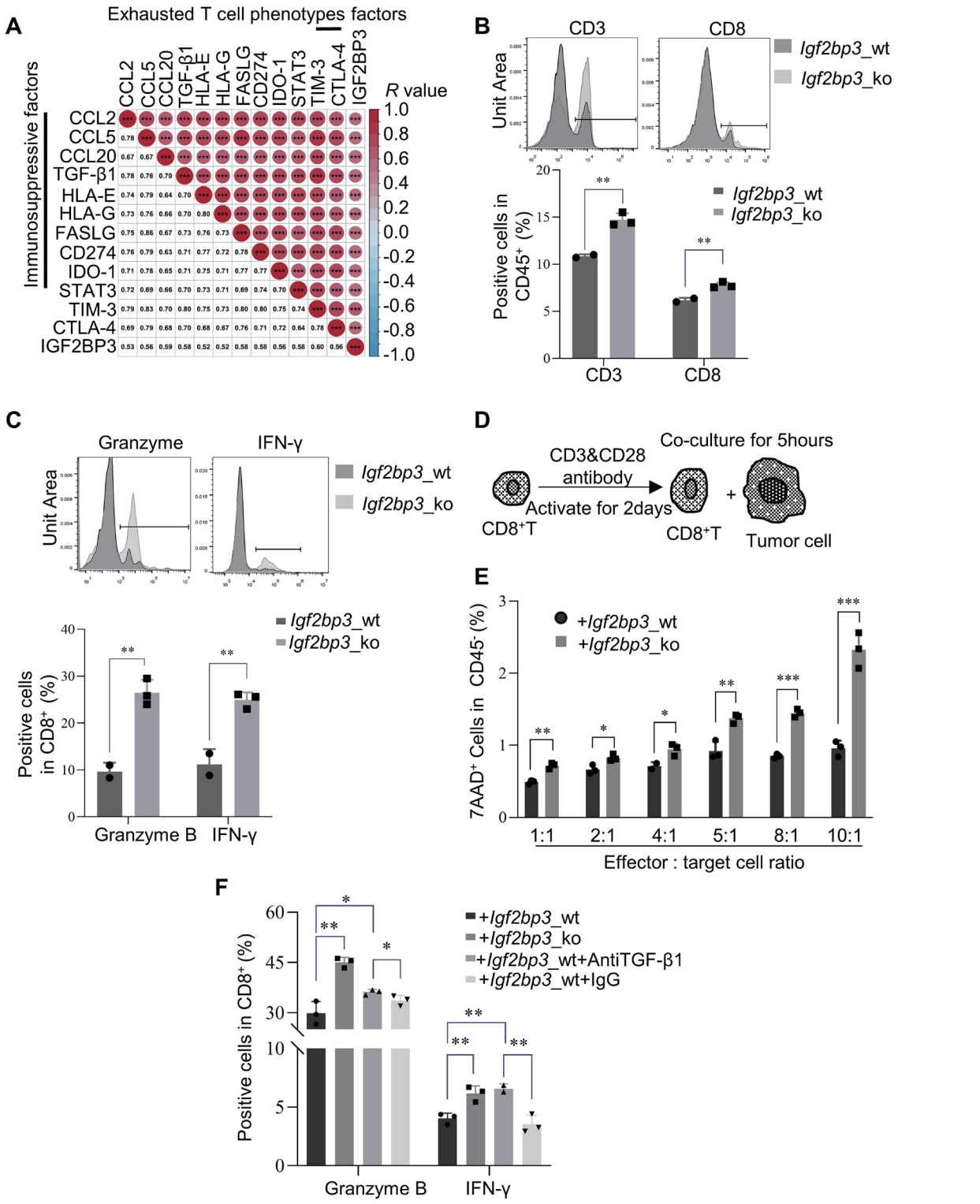

Fig. 5. IGF2BP3 inhibits the activation of CD8⁺ T cells by promoting the secretion of TGF-β1. (A) The graph shows the correlations between IGF2BP3 and immunosuppressive markers in the TCGA HCC dataset (*n*=371). (B, C) Splenocytes were isolated from C57BL/6J mice and cocultured with *Igf2bp3*_wt and *Igf2bp3*_ko cells for 48h. Flow cytometry analysis of the proportion of CD3⁺ T, CD8⁺ T cells (B) and the expression of granzyme B, IFN-γ in CD8⁺ T cells at the end of coculture (C). (D, F) CD8⁺ T cells were isolated from splenocytes of C57BL/6J mice and activated by treatment with anti-CD3/CD28 antibody for 2 days (D). Activated CD8⁺ T cells were cocultured with *Igf2bp3*_wt or *Igf2bp3*_ko cells at ratios of 1:1, 2:1, 4:1, 5:1, 8:1, or 10:1. Cell death analysis was conducted by flow cytometry (E). Activated CD8⁺ T cells were cocultured with *Igf2bp3*_wt, *Igf2bp3*_ko cells for 2 days; TGF-β1 neutralizing antibody (1 μg/mL) was added to cocultures. The percentage of granzyme B and IFN-γ were analyzed by flow cytometry (F). Data are mean±SD. **p*<0.05, ***p*<0.01, ****p*<0.001.

mice were isolated 18 days after inoculation of tumor cells. After coculture with tumor cells for 48 h, the proportion of $CD3^+$ T and $CD8^+$ T cells in the *Igf2bp3*_ko tumor cell group was found to be higher than that in the *Igf2bp3*_wt group ($p<0.01$; Fig. 5B). Moreover, granzyme B and IFN-γ secreted by $CD8^+$ T cells was significantly increased in the *Igf2bp3*_ko group ($p<0.01$; Fig. 5C), indicating that tumor cell-derived IGF2BP3 inhibited the activation of $CD8^+$ T cells. Furthermore, we sorted $CD8^+$ T cells and cocultured them with *Igf2bp3*_wt or *Igf2bp3*_ko cells after activation by anti-CD3 and anti-CD28 (Fig. 5D). The $CD8^+$ T/tumor cell ratios were 1:1, 2:1, 4:1, 5:1, 8:1, or 10:1. Increased $7AAD^+$ tumor cells were detected in *Igf2bp3*_ko group in all experimental settings (Fig. 5C–E). In addition, both granzyme B ($p<0.01$) and IFN-γ ($p<0.01$) generated by $CD8^+$ T cells were increased in the group cocultured with *Igf2bp3*_ko cells compared with the *Igf2bp3*_wt group (Fig. 5F). When TGF-β1 neutralizing antibody was added into the *Igf2bp3*_wt group, the levels of granzyme B ($p<0.05$) and IFN-γ ($p<0.01$) secreted by $CD8^+$ T cells were elevated compared with the *Igf2bp3*_wt group (Fig. 5F). Collectively, the findings suggest that IGF2BP3 inhibited activation of $CD8^+$ T cells by promoting the secretion of TGF-β1.

IGF2BP3 directly binds to the mRNA of Ccl5 or Tgf-β1

As IGF2BP3 is an RNA binding protein (RBP), we sought to investigate whether IGF2PB3 directly binds with *Ccl5* or *Tgf-β1* mRNA. We used the website RBP suite database (http://www.csbio.sjtu.edu.cn/bioinf/RBPsuite/), which can predict RBP binding site in RNA. All the predicted binding sites are shown in Figure 6A–B. Supplementary Table 2 shows the sequences of which score was greater than 0.5. RIP-PCR assays found two sequences, *Ccl5*-7 and *Tgf-β1*-28, were enriched in IGF2BP3 immunoprecipitated products (Fig. 6C and Supplementary Fig. 2A–B), which was confirmed by analysis of relative gray values ($p<0.001$; Fig. 6D). Enrichment of the two fragments (*Ccl5*-7 and *Tgf-β1*-28) were also validated by qRT-PCR ($p<0.001$; Fig. 6E). mNeptune-based TriFC is a system used to monitor mRNA and protein interactions.[23] If the candidate RBP interacts with the RNA sequence of interest, re-association of the two mNeptune fragments produces a red TriFC signal. pECFP-C1-MS2-*Ccl5*-7, pECFP-C1-MS2-*Tgf-β1*-28, and pECFP-C1-ms2 (control) were transfected into 293T cells with p*Igf2bp3*-MN155 and pMC 156-MCP plasmids. We observed significant red TriFC fluorescence signals in 293T cells transfected with pECFP-C1-MS2-*Ccl5*-7 or pECFP-C1-MS2-*Tgf-β1*-28 compared with the control group (Fig. 6F). Collectively, the findings strongly indicate that IGF2BP3 directly bound to the mRNA of *Ccl5* or *Tgf-β1*.

Combination of Igf2bp3 knockout and CD47 blockade has synergistic antitumorigenic effects in mouse HCC model

CD47 neutralizing antibodies have been used to enhance phagocytosis, a key function of macrophages, for HCC treatment.[27] Hence, we hypothesized that the combined approach of *Igf2bp3* knockout and CD47 neutralizing antibody would not only accelerate macrophage phagocytosis, but also hinder M2-polarization and elicit better activation of $CD8^+$ T cell. The results demonstrated that knockout of *Igf2bp3* combined with anti-CD47 therapy led to significantly slower tumor growth (Fig. 7A). Both the final tumor volume and weight were smallest in the combination treatment group (Fig. 7B–C). The findings strongly suggest synergistic antitumorigenicity of Igf2bp3 inhibition and blockade of CD47. Overall, our study demonstrates that IGF2BP3 facilitated the infiltration and M2-polarization of macrophages and inhibited $CD8^+$ T-cell activation. The activity was the result of the binding of IGF2BP3 to RNA fragments of *Ccl5* and *Tgf-β1*, leading to an increased secretion of CCL5 and TGF-β1 (Fig. 7D).

Discussion

There were three main study findings: (1) IGF2BP3 was found to promote infiltration of macrophages by up-regulating CCL5; (2) IGF2BP3 induced M2 polarization of macrophages and inhibited $CD8^+$ T-cell activation by increasing the expression of TGF-β1; (3) IGF2BP3 was found to directly bind to *Ccl5* or *Tgf-β1* mRNA. The CCL5/CCR5 axis has been shown to be intricately involved in cancer progression through various mechanisms such as by promoting tumor growth and invasiveness, remodeling of the extracellular matrix, expansion of cancer stem cells, resistance to drugs, angiogenesis, and polarization of immunosuppressive macrophage.[28] Blocking this axis with anti-CCR5 induced repolarization of macrophages with antitumor effects.[29] In an $EGFR^{L858R}$-induced mouse lung cancer model, inhibition of TP53 enhanced the polarization of M2 macrophages by increasing the expression of CCL5.[30] CCL5 is also known to stimulate macrophage migration and recruitment.[24] Oncolytic virus expressing fusion protein of cetuximab and CCL5 enhanced the migration and activation of immune cells including macrophages, which improved the therapeutic effect against solid tumors.[31] In our study, IGF2BP3 was found to promote CCL5 secretion by binding to *Ccl5* mRNA, thereby inducing macrophage infiltration of the tumor.

TGFβ signaling is one of the canonical pathways whose abnormality drives carcinogenesis.[32] It was shown to be an important factor in the induction of epithelial-mesenchymal transition.[33] It was also shown to facilitate cancer progression by promoting immunosuppression and inducing M2 polarization.[34–36] Inhibitor or antibody against TGFβ showed promising antitumor activities.[37] Our results also indicated that IGF2BP3 promoted TGF-β1 secretion in tumor cells, which polarized macrophages toward M2 phenotype. Thus, to the best of our knowledge, this is the first study to identify that IGF2BP3 acts on both macrophages and $CD8^+$ T cells by binding to CCL5 and TGF-β1 in the immune microenvironment of HCC mouse model. Given the broad role of CCL5 and TGF-β1, other functions of IGF2BP3 in HCC immune microenvironment remain to be further explored.

As an RBP, IGF2BP3 has been widely shown to promote the malignant phenotype of tumor cells, but its effects on immune cells are not well characterized in the contemporary literature. A study at the pan-cancer level found that IGF2BP3 may be related to macrophage infiltration of tumors.[38] In a study investigating spontaneous abortion, IGF2BP3 was found to promote M2 polarization of macrophages.[39] IGF2BP3 facilitated immune evasion of cancerous cells by downregulating the NKG2D ligand ULBP2 in a direct manner.[40] The findings suggested the ability of IGF2BP3 to influence the immune microenvironment. In this study, we investigated the impact of IGF2BP3 on the immune microenvironment of HCC and found that IGF2BP3 promoted the infiltration and M2 polarization of macrophages and inhibited the activation of $CD8^+$ T cells. In previous studies, IGF2BP3 in HCC mainly promoted various malignant phenotypes of the tumor cell itself.[41] Our study extends the role of IGF2BP3 to regulating the functions of immune cells, providing a theoretical basis for the subsequent exploration of IGF2BP3 in the immune microenvironment and providing new insights for the development of immunotherapy for HCC.

As for the molecular mechanisms, it has been reported

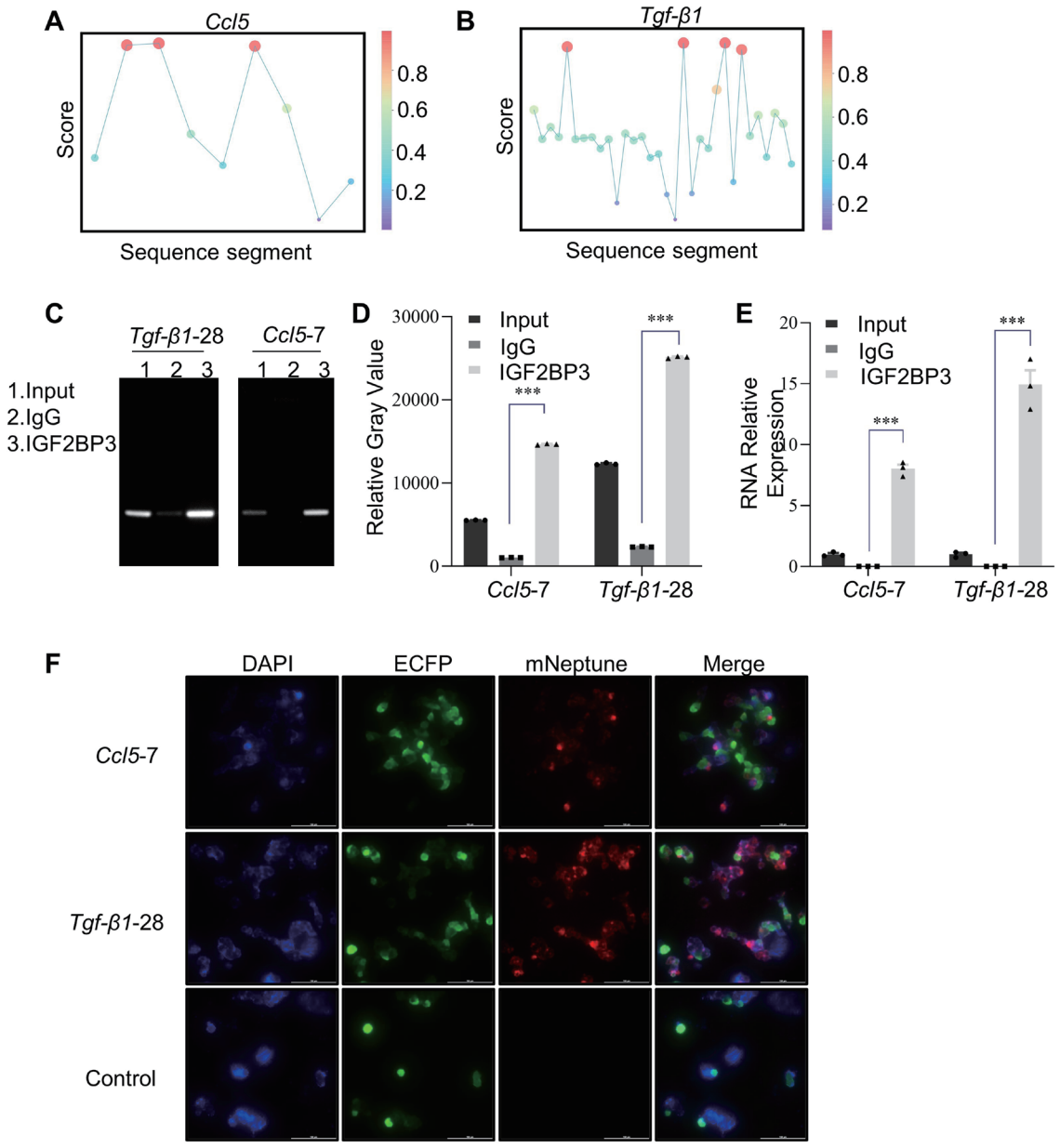

Fig. 6. IGF2BP3 directly binds to the mRNA of *Ccl5* or *Tgf-β1*. (A, B) Binding site analysis of IGF2BP3 around the *Ccl5* and *Tgf-β1* mRNA using the RBP suite database. (C–E) RIP experiment was performed using IGF2BP3 antibodies followed by PCR (C, D) and qRT-PCR (E) with specific primers of *Ccl5* and *Tgf-β1* mRNA. (F) Detecting the binding between IGF2BP3 and mRNA of *Ccl5* or *Tgf-β1* in 293T cells using the TriFC system. pECFP-C1-MS2-*Ccl5*-7 (*Ccl5*-7), pECFP-C1-MS2-*Tgf-β1*-28 (*Tgf-β1*-28) and pECFP-C1-ms2 (control) were transfected into 293T cells, with p*Igf2bp3*-MN155 and pMC 156-MCP plasmids. Representative pictures of immunofluorescence. Scale bar=100 μm. Data are mean±SD. ***p<0.001. RBP, RNA binding protein; RIP, RNA immunoprecipitation.

that IGF2BP3 has an important role in tumor development by regulating mRNA stability.[42] In colorectal cancer, IGF2BP3 was shown to enhance the expression of MEKK1 by stabilizing the mRNA by directly binding its 3′-UTR, activating the MEK1/ERK signaling pathway.[43] In addition to promoting RNA stability, IGF2BP3 also reduces the stability of certain RNAs. For example, IGF2BP3 binds to EIF4E-BP2 mRNA leading to its degradation, thereby promoting EIF4E-mediated translational activation.[44] In our study, IGF2BP3 was found to directly bind to the mRNA of *Ccl5* and *Tgf-β1*. The regulatory mechanism by which IGF2BP3 affects the secretion of both molecules after binding to their mRNAs is a focus of our subsequent studies. Our preliminary results suggested that IGF2BP3 enhanced the translation of *Ccl5* or *Tgf-β1*, ultimately promoting their secretion. However, more experimental evidence is needed to confirm this conclusion.

Immunotherapy has shown promising results in the treatment of HCC. However, despite the success of combination immunotherapies in improving clinical response rates, nearly 70% of patients are unresponsive to such treatments, and the underlying mechanism remains unclear.[45] Therefore, investigating the immune microenvironment of HCC is imperative for developing effective treatments. IGF2BP3 is strongly expressed in tumors but weakly expressed in normal tissues,

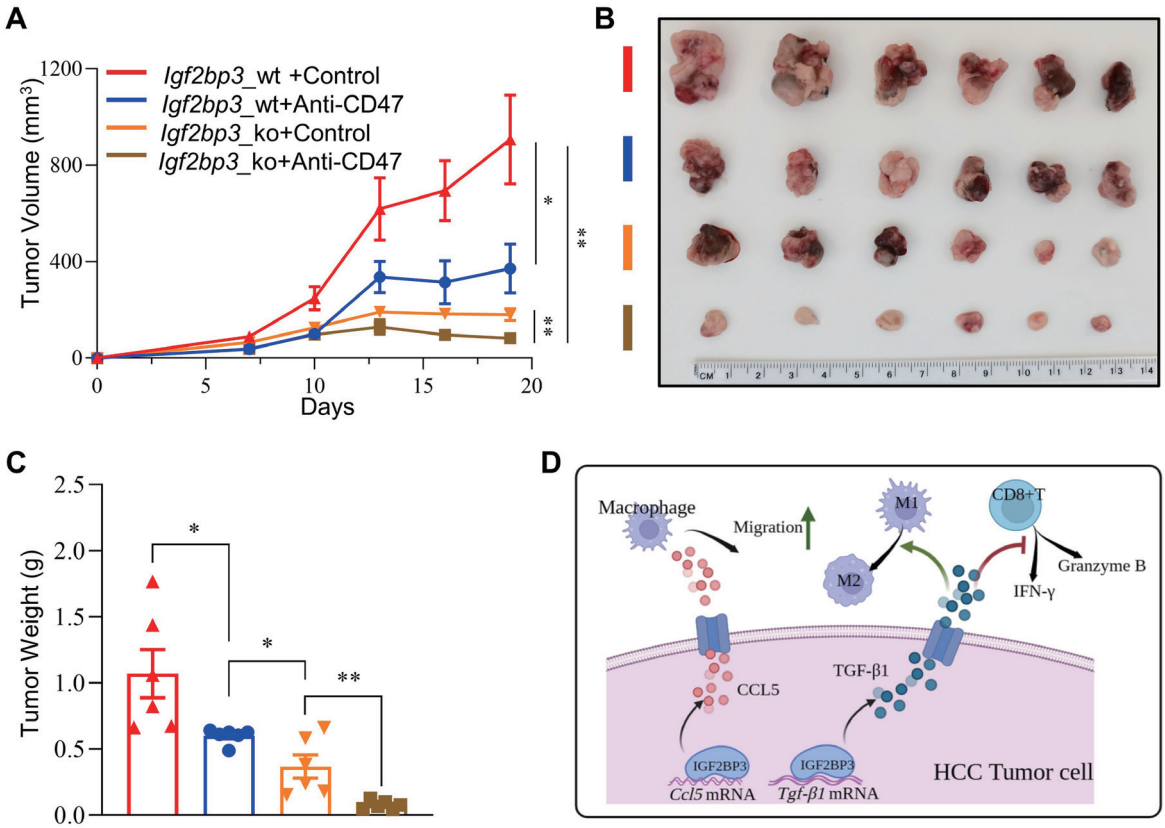

Fig. 7. Combined treatment with *Igf2bp3* knockout and CD47 blockade has synergistic antitumorigenic effects in the mouse HCC model. (A–C) *Igf2bp3*_wt and *Igf2bp3*_ko cells were subcutaneously injected into male C57BL/6J mice. From day 7, mice were administered intraperitoneal injections of anti-CD47 neutralizing antibodies (400 μg/mouse, 100 μL) every 3 days or an equal volume of PBS. The graph shows tumor volumes on days 7, 10, 13, 16, and 19 (A). Mice were sacrificed on day 20. Image of tumor from the four groups (B); bar chart shows tumor weight (C). (D) Schematic illustration showing of IGF2BP3 promotion of macrophage infiltration, M2 polarization, inhibition of $CD8^+$ T-cell activation in HCC. This follows the binding of IGF2BP3 to the RNA fragments of *Ccl5* and *Tgf-β*, leading to increased secretion of CCL5 and TGF-β1. Figure created with BioRender.com. Data are mean±SD. *p<0.05, **p<0.01. HCC, hepatocellular carcinoma; PBS, phosphate buffered saline.

making it a potential therapeutic target.[41] Additionally, CD47 expression is upregulated in HCC, and anti-CD47 antibody can induce macrophage mediated phagocytosis.[46–48] In our study, IGF2BP3 promoted M2 polarization of macrophages in HCC. Therefore, it is expected that the combination of CD47 neutralizing antibody and IGF2BP3 inhibition may reduce M2 polarization of macrophages and promote macrophage phagocytosis. Our results suggest that IGF2BP3 inhibition combined with anti-CD47 antibody improved the therapeutic effectiveness against tumors. Although our combined treatment strategy was effective in the Hepa1-6 xenograft tumor mouse model, further studies are required to determine the effectiveness of this treatment in other models.

Conclusions

In summary, we uncovered two novel targets of IGF2BP3 through which IGF2BP3 mediated macrophage infiltration, M2 polarization, and suppressed $CD8^+$ T-cell activation in the liver cancer mouse model. Moreover, the combination of anti-CD47 treatment and IGF2BP3 deficiency effectively decreased the tumor load in the Hepa1-6 xenograft tumor mouse model.

Acknowledgments

The authors would like to thank Zongqiang Cui (State Key Laboratory of Virology, Wuhan Institute of Virology, Chinese Academy of Sciences, Wuhan 430071, China) for providing the original plasmid of the TriFC system. We also thank Prof. Yunping Luo (Institute of Basic Medical Sciences, Chinese Academy of Medical Sciences, School of Basic Medicine, Peking Union Medical College, Beijing 100730, China) for the support to this project.

Funding

This work was supported by the National Natural Science Foundation of China (81601374), the Fundamental Research Funds for the Central Universities (3332022181), and the Bilateral Inter-Governmental S&T Cooperation Project from the Ministry of Science and Technology of China (2018YFE0114300).

Conflict of interest

The authors have no conflict of interests related to this publication.

Author contributions

ZD designed the project. LM performed the experiments and analyzed the data with JJ, QS and CC. The manuscript was drafted by LM and revised by ZD. All authors contributed to the article and approved the submitted version.

Ethical statement

The animal study was reviewed and approved by institutional review board of Institute of Basic Medical Sciences, Chinese Academy of Medical Sciences.

Data sharing statement

The original contributions presented in the study are included in the article/supplementary material. Further inquiries can be directed to the corresponding authors.

References

[1] Sangro B, Sarobe P, Hervas-Stubbs S, Melero I. Advances in immunotherapy for hepatocellular carcinoma. Nat Rev Gastroenterol Hepatol 2021;18(8):525–543. doi:10.1038/s41575-021-00438-0, PMID:33850328.

[2] Jenne CN, Kubes P. Immune surveillance by the liver. Nat Immunol 2013;14(10):996–1006. doi:10.1038/ni.2691, PMID:24048121.

[3] Yeung OW, Lo CM, Ling CC, Qi X, Geng W, Li CX, *et al*. Alternatively activated (M2) macrophages promote tumour growth and invasiveness in hepatocellular carcinoma. J Hepatol 2015;62(3):607–616. doi:10.1016/j.jhep.2014.10.029, PMID:25450711.

[4] Wang C, Ma C, Gong L, Guo Y, Fu K, Zhang Y, *et al*. Macrophage Polarization and Its Role in Liver Disease. Front Immunol 2021;12:803037. doi:10.3389/fimmu.2021.803037, PMID:34970275.

[5] Lv Y, Wang Z, Yuan K. Role of Noncoding RNAs in the Tumor Immune Microenvironment of Hepatocellular Carcinoma. J Clin Transl Hepatol 2023;11(3):682–694. doi:10.14218/JCTH.2022.00412, PMID:36969884.

[6] Lin EY, Li JF, Gnatovskiy L, Deng Y, Zhu L, Grzesik DA, *et al*. Macrophages regulate the angiogenic switch in a mouse model of breast cancer. Cancer Res 2006;66(23):11238–11246. doi:10.1158/0008-5472.CAN-06-1278, PMID:17114237.

[7] Qian B, Deng Y, Im JH, Muschel RJ, Zou Y, Li J, *et al*. A distinct macrophage population mediates metastatic breast cancer cell extravasation, establishment and growth. PLoS One 2009;4(8):e6562. doi:10.1371/journal.pone.0006562, PMID:19668347.

[8] Talmadge JE, Donkor M, Scholar E. Inflammatory cell infiltration of tumors: Jekyll or Hyde. Cancer Metastasis Rev 2007;26(3-4):373–400. doi:10.1007/s10555-007-9072-0, PMID:17717638.

[9] Li LB, Yang L, Xie GQ, Zhou XC, Shen XB, Xu QL, *et al*. The modulation relationship of genomic pattern of intratumor heterogeneity and immunity microenvironment heterogeneity in hepatocellular carcinoma. Oncol Lett 2020;20(5):233. doi:10.3892/ol.2020.12096, PMID:32968455.

[10] Lamagna C, Aurrand-Lions M, Imhof BA. Dual role of macrophages in tumor growth and angiogenesis. J Leukoc Biol 2006;80(4):705–713. doi:10.1189/jlb.1105656, PMID:16864600.

[11] Wang PF, Wang X, Liu M, Zeng Z, Lin C, Xu W, *et al*. The Oncogenic Functions of Insulin-like Growth Factor 2 mRNA-Binding Protein 3 in Human Carcinomas. Curr Pharm Des 2020;26(32):3939–3954. doi:10.2174/1381612826666200413080936, PMID:32282295.

[12] Gong Y, Woda BA, Jiang Z. Oncofetal protein IMP3, a new cancer biomarker. Adv Anat Pathol 2014;21(3):191–200. doi:10.1097/PAP.0000000000000021, PMID:24713990.

[13] Monk D, Bentley L, Beechey C, Hitchins M, Peters J, Preece MA, *et al*. Characterisation of the growth regulating gene IMP3, a candidate for Silver-Russell syndrome. J Med Genet 2002;39(8):575–581. doi:10.1136/jmg.39.8.575, PMID:12161597.

[14] Fawzy IO, Hamza MT, Hosny KA, Esmat G, Abdelaziz AI. Abrogating the interplay between IGF2BP1, 2 and 3 and IGF1R by let-7i arrests hepatocellular carcinoma growth. Growth Factors 2016;34(1-2):42–50. doi:10.3109/08977194.2016.1169532, PMID:27126374.

[15] Fawzy IO, Hamza MT, Hosny KA, Esmat G, El Tayebi HM, Abdelaziz AI. miR-1275: A single microRNA that targets the three IGF2-mRNA-binding proteins hindering tumor growth in hepatocellular carcinoma. FEBS Lett 2015;589(17):2257–2265. doi:10.1016/j.febslet.2015.06.038, PMID:26160756.

[16] Jeng YM, Chang CC, Hu FC, Chou HY, Kao HL, Wang TH, *et al*. RNA-binding protein insulin-like growth factor II mRNA-binding protein 3 expression promotes tumor invasion and predicts early recurrence and poor prognosis in hepatocellular carcinoma. Hepatology 2008;48(4):1118–1127. doi:10.1002/hep.22459, PMID:18802962.

[17] Jiang W, Cheng X, Wang T, Song X, Zheng Y, Wang L. LINC00467 promotes cell proliferation and metastasis by binding with IGF2BP3 to enhance the mRNA stability of TRAF5 in hepatocellular carcinoma. J Gene Med 2020;22(3):e3134. doi:10.1002/jgm.3134, PMID:31656043.

[18] Li Z, Zhang J, Liu X, Li S, Wang Q, Di C, *et al*. The LINC01138 drives malignancies via activating arginine methyltransferase 5 in hepatocellular carcinoma. Nat Commun 2018;9(1):1572. doi:10.1038/s41467-018-04006-0, PMID:29679004.

[19] Yang Z, Wang T, Wu D, Min Z, Tan J, Yu B. RNA N6-methyladenosine reader IGF2BP3 regulates cell cycle and angiogenesis in colon cancer. J Exp Clin Cancer Res 2020;39(1):203. doi:10.1186/s13046-020-01714-8, PMID:32993738.

[20] Li M, Zhang L, Ge C, Chen L, Fang T, Li H, *et al*. An isocorydine derivative (d-ICD) inhibits drug resistance by downregulating IGF2BP3 expression in hepatocellular carcinoma. Oncotarget 2015;6(28):25149–25160. doi:10.18632/oncotarget.4438, PMID:26327240.

[21] Huang W, Zhu L, Huang H, Li Y, Wang G, Zhang C. IGF2BP3 overexpression predicts poor prognosis and correlates with immune infiltration in bladder cancer. BMC Cancer 2023;23(1):116. doi:10.1186/s12885-022-10353-5, PMID:36732736.

[22] Li D, Li K, Zhang W, Yang KW, Mu DA, Jiang GJ, *et al*. The m6A/m5C/m1A Regulated Gene Signature Predicts the Prognosis and Correlates With the Immune Status of Hepatocellular Carcinoma. Front Immunol 2022;13:918140. doi:10.3389/fimmu.2022.918140, PMID:35833147.

[23] Han Y, Wang S, Zhang Z, Ma X, Li W, Zhang X, *et al*. In vivo imaging of protein-protein and RNA-protein interactions using novel far-red fluorescence complementation systems. Nucleic Acids Res 2014;42(13):e103. doi:10.1093/nar/gku408, PMID:24813442.

[24] Zong C, Meng Y, Ye F, Yang X, Li R, Jiang J, *et al*. AIF1(+) CSF1R(+) MSCs, induced by TNF-alpha, act to generate an inflammatory microenvironment and promote hepatocarcinogenesis. Hepatology 2022. doi:10.1002/hep.32738, PMID:35989499.

[25] Liu L, Cheng M, Zhang T, Chen Y, Wu Y, Wang Q. Mesenchymal stem cell-derived extracellular vesicles prevent glioma by blocking M2 polarization of macrophages through a miR-744-5p/TGFB1-dependent mechanism. Cell Biol Toxicol 2022;38(4):649–665. doi:10.1007/s10565-021-09652-7, PMID:34978010.

[26] de Streel G, Lucas S. Targeting immunosuppression by TGF-beta1 for cancer immunotherapy. Biochem Pharmacol 2021;192:114697. doi:10.1016/j.bcp.2021.114697, PMID:34302795.

[27] Lo J, Lau EY, So FT, Lu P, Chan VS, Cheung VC, *et al*. Anti-CD47 antibody suppresses tumour growth and augments the effect of chemotherapy treatment in hepatocellular carcinoma. Liver Int 2016;36(5):737–745. doi:10.1111/liv.12963, PMID:26351778.

[28] Aldinucci D, Borghese C, Casagrande N. The CCL5/CCR5 Axis in Cancer Progression. Cancers (Basel) 2020;12(7):1765. doi:10.3390/cancers12071765, PMID:32630699.

[29] Halama N, Zoernig I, Berthel A, Kahlert C, Klupp F, Suarez-Carmona M, *et al*. Tumoral Immune Cell Exploitation in Colorectal Cancer Metastases Can Be Targeted Effectively by Anti-CCR5 Therapy in Cancer Patients. Cancer Cell 2016;29(4):587–601. doi:10.1016/j.ccell.2016.03.005, PMID:27070705.

[30] Chen YC, Young MJ, Chang HP, Liu CY, Lee CC, Tseng YL, *et al*. Estradiol-mediated inhibition of DNMT1 decreases p53 expression to induce M2-macrophage polarization in lung cancer progression. Oncogenesis 2022;11(1):25. doi:10.1038/s41389-022-00397-4, PMID:35589688.

[31] Tian L, Xu B, Chen Y, Li Z, Wang J, Zhang J, *et al*. Specific targeting of glioblastoma with an oncolytic virus expressing a cetuximab-CCL5 fusion protein via innate and adaptive immunity. Nat Cancer 2022;3(11):1318–1335. doi:10.1038/s43018-022-00448-0, PMID:36357700.

[32] Sanchez-Vega F, Mina M, Armenia J, Chatila WK, Luna A, La KC, *et al*. Oncogenic Signaling Pathways in The Cancer Genome Atlas. Cell 2018;173(2):321–337.e310. doi:10.1016/j.cell.2018.03.035, PMID:29625050.

[33] Lamouille S, Xu J, Derynck R. Molecular mechanisms of epithelial-mesenchymal transition. Nat Rev Mol Cell Biol 2014;15(3):178–196. doi:10.1038/nrm3758, PMID:24556840.

[34] Peng P, Zhu H, Liu D, Chen Z, Zhang X, Guo Z, *et al*. TGFBI secreted by tumor-associated macrophages promotes glioblastoma stem cell-driven tumor growth via integrin alphavbeta5-Src-Stat3 signaling. Theranostics 2022;12(9):4221–4236. doi:10.7150/thno.69605, PMID:35673564.

[35] Batlle E, Massague J. Transforming Growth Factor-beta Signaling in Immunity and Cancer. Immunity 2019;50(4):924–940. doi:10.1016/j.immuni.2019.03.024, PMID:30995507.

[36] Mariathasan S, Turley SJ, Nickles D, Castiglioni A, Yuen K, Wang Y, *et al*. TGFbeta attenuates tumour response to PD-L1 blockade by contributing to exclusion of T cells. Nature 2018;554(7693):544–548. doi:10.1038/nature25501, PMID:29443960.

[37] Morris JC, Tan AR, Olencki TE, Shapiro GI, Dezube BJ, Reiss M, *et al*. Phase I study of GC1008 (fresolimumab): a human anti-transforming growth factor-beta (TGFbeta) monoclonal antibody in patients with advanced malignant melanoma or renal cell carcinoma. PLoS One 2014;9(3):e90353. doi:10.1371/journal.pone.0090353, PMID:24618589.

[38] Shao W, Zhao H, Zhang S, Ding Q, Guo Y, Hou K, *et al*. A pan-cancer landscape of IGF2BPs and their association with prognosis, stemness and tumor immune microenvironment. Front Oncol 2022;12:1049183. doi:10.3389/fonc.2022.1049183, PMID:36686749.

[39] Zhang Y, Dai F, Yang D, Zheng Y, Zhu R, Wu M, *et al*. Deletion of Insulin-like growth factor II mRNA-binding protein 3 participates in the pathogenesis of recurrent spontaneous abortion by inhibiting IL-10 secretion and inducing M1 polarization. Int Immunopharmacol 2023;114:109473. doi:10.1016/j.intimp.2022.109473, PMID:36463698.

[40] Schmiedel D, Tai J, Yamin R, Berhani O, Bauman Y, Mandelboim O. The RNA binding protein IMP3 facilitates tumor immune escape by downregulating the stress-induced ligands ULPB2 and MICB. Elife 2016;5:e13426. doi:10.7554/eLife.13426, PMID:26982091.

[41] Mancarella C, Scotlandi K. IGF2BP3 From Physiology to Cancer: Novel Discoveries, Unsolved Issues, and Future Perspectives. Front Cell Dev Biol 2019;7:363. doi:10.3389/fcell.2019.00363, PMID:32010687.

[42] Nielsen FC, Nielsen J, Kristensen MA, Koch G, Christiansen J. Cytoplasmic trafficking of IGF-II mRNA-binding protein by conserved KH domains. J Cell Sci 2002;115(Pt 10):2087–2097. doi:10.1242/jcs.115.10.2087, PMID:11973350.

[43] Zhang M, Zhao S, Tan C, Gu Y, He X, Du X, *et al*. RNA-binding protein IMP3 is a novel regulator of MEK1/ERK signaling pathway in the progression of colorectal Cancer through the stabilization of MEKK1 mRNA. J Exp Clin Cancer Res 2021;40(1):200. doi:10.1186/s13046-021-01994-8, PMID:341

54626.
[44] Mizutani R, Imamachi N, Suzuki Y, Yoshida H, Tochigi N, Oonishi T, *et al*. Oncofetal protein IGF2BP3 facilitates the activity of proto-oncogene protein eIF4E through the destabilization of EIF4E-BP2 mRNA. Oncogene 2016;35(27):3495–3502. doi:10.1038/onc.2015.410, PMID:26522719.
[45] Wang K, Wang C, Jiang H, Zhang Y, Lin W, Mo J, *et al*. Combination of Ablation and Immunotherapy for Hepatocellular Carcinoma: Where We Are and Where to Go. Front Immunol 2021;12:792781. doi:10.3389/fimmu.2021.792781, PMID:34975896.
[46] Chao MP, Alizadeh AA, Tang C, Myklebust JH, Varghese B, Gill S, *et al*. Anti-CD47 antibody synergizes with rituximab to promote phagocytosis and eradicate non-Hodgkin lymphoma. Cell 2010;142(5):699–713. doi:10.1016/j.cell.2010.07.044, PMID:20813259.
[47] Jaiswal S, Jamieson CH, Pang WW, Park CY, Chao MP, Majeti R, *et al*. CD47 is upregulated on circulating hematopoietic stem cells and leukemia cells to avoid phagocytosis. Cell 2009;138(2):271–285. doi:10.1016/j.cell.2009.05.046, PMID:19632178.
[48] Majeti R, Chao MP, Alizadeh AA, Pang WW, Jaiswal S, Gibbs KD Jr, *et al*. CD47 is an adverse prognostic factor and therapeutic antibody target on human acute myeloid leukemia stem cells. Cell 2009;138(2):286–299. doi:10.1016/j.cell.2009.05.045, PMID:19632179.